

# The Cotranslational Contacts between Ribosome-bound Nascent Polypeptides and the Subunits of the Hetero-oligomeric Chaperonin TRiC Probed by Photocross-linking\*

Received for publication, April 15, 2005, and in revised form, May 27, 2005  
Published, JBC Papers in Press, May 30, 2005, DOI 10.1074/jbc.M504110200

Stephanie A. Etchells<sup>‡§</sup>, Anne S. Meyer<sup>¶</sup>, Alice Y. Yam<sup>¶</sup>, Anne Roobol<sup>||</sup>, Yiwei Miao<sup>\*\*</sup>,  
Yuanlong Shao<sup>\*\*</sup>, Martin J. Carden<sup>||</sup>, William R. Skach<sup>‡‡</sup>, Judith Frydman<sup>¶</sup>,  
and Arthur E. Johnson<sup>‡\*\*§§¶¶</sup>

From the Departments of <sup>‡</sup>Biochemistry and Biophysics and <sup>§§</sup>Chemistry, Texas A&M University, College Station, Texas 77843, the <sup>¶¶</sup>Department of Biological Sciences, Stanford University, Stanford, California 94305, the <sup>||</sup>Department of Biosciences, University of Kent, Canterbury CT2 7NJ, United Kingdom, the <sup>\*\*</sup>Department of Medical Biochemistry and Genetics, Texas A&M University Health Science Center, College Station, Texas 77843-1114, and the <sup>‡‡</sup>Division of Molecular Medicine, Oregon Health and Sciences University, Portland, Oregon 97201

The hetero-oligomeric eukaryotic chaperonin TRiC (TCP-1-ring complex, also called CCT) interacts cotranslationally with a diverse subset of newly synthesized proteins, including actin, tubulin, and luciferase, and facilitates their correct folding. A photocross-linking approach has been used to map the contacts between individual chaperonin subunits and ribosome-bound nascent chains of increasing length. Whereas a cryo-EM study suggests that chemically denatured actin interacts with only two TRiC subunits ( $\delta$  and either  $\beta$  or  $\epsilon$ ), actin and luciferase chains photocross-link to at least six TRiC subunits ( $\alpha$ ,  $\beta$ ,  $\delta$ ,  $\epsilon$ ,  $\xi$ , and  $\theta$ ) at different stages of translation. Furthermore, the photocross-linking of actin, but not luciferase, nascent chains to TRiC subunits  $\zeta$  and  $\theta$  was length-dependent. In addition, a single photoreactive probe incorporated at a unique site in actin nascent chains of different lengths reacted covalently with multiple TRiC subunits, thereby indicating that the nascent chain samples the polypeptide binding sites of different subunits. We conclude that elongating actin and luciferase nascent chains contact multiple TRiC subunits upon emerging from the ribosome, and that the TRiC subunits contacted by nascent actin change as it elongates and starts to fold.

co-chaperonin complex such as GroES for productive folding, and are found in prokaryotes, mitochondria, and chloroplasts (1, 5). GroEL is thought to function primarily in a post-translational manner (1–3), although cotranslational interactions have been reported for some proteins (6). Type II chaperonins are found in Archaea and eukaryotes, are hetero-oligomeric, and do not require a GroES-like cofactor (4, 7). The eukaryotic chaperonin named TRiC<sup>1</sup> (for TCP-1 ring complex) or CCT (for chaperonin containing TCP1) consists of eight different, yet homologous, subunits per ring that are designated either  $\alpha$ – $\theta$  or 1–8. Based on an analysis of chaperonin subcomplexes (8), a clockwise order for the arrangement of subunits in the ring has been proposed to be, moving clockwise,  $\alpha/1$ ,  $\epsilon/5$ ,  $\zeta/6$ ,  $\beta/2$ ,  $\gamma/3$ ,  $\theta/8$ ,  $\delta/4$ , and  $\eta/7$ .

All TRiC subunits are essential for viability in yeast (4), and this raises a fundamental question: why did TRiC evolve different subunits if prokaryotes can mediate folding with homo-oligomeric chaperonins? One possibility is that certain TRiC subunits or combinations of subunits interact with substrates that have specific structural features or motifs, and that eight unique subunits provide a mechanism for accommodating a wider variety of substrates (9, 10). But in fact, little is known about how TRiC interacts with its substrates.

Several studies have examined how purified TRiC interacts *in vitro* with chemically denatured substrates, including actin and actin-derived peptides (10, 11). For instance, cryo-EM studies of binary complexes made by incubating purified and chemically denatured actin with purified TRiC suggested that TRiC-bound actin is in close proximity to only two subunits,  $\delta$  and either  $\beta$  or  $\epsilon$  (9). These experiments further proposed that subdomain 2 of actin (amino acids 33–78) bound only to the  $\delta$  subunit, whereas domain 4 (amino acids 179–261) bound to either subunit  $\beta$  or  $\epsilon$ . Yet these approaches have two significant drawbacks. First, because high-resolution cryo-EM analysis relies on averaging particles that contain electron-dense material within the cavity, these experiments can only detect chaperonin proximity to compact, well defined, and stable structures in the substrate. Yet TRiC binding sites in the substrate may localize to flexible regions that are either not resolved or are averaged out during the single particle reconstruction, and hence are not seen. Second, analyzing chemically unfolded polypeptides does not appear to reproduce what happens *in*

Double-ring chaperonin complexes play a fundamental role in cellular protein folding (1–4). Based on their ability to bind unfolded polypeptides within their ring cavities, chaperonins prevent off-pathway reactions and promote productive protein folding to the native state in a highly cooperative, ATP-dependent manner. Type I chaperonins such as *Escherichia coli* GroEL are generally homo-oligomeric, require a ring-shaped

\* This work was supported by National Institutes of Health Grants GM26494 (to A. E. J.), GM56433 (to J. F.), GM53457 (to W. S.), and DK51818 (to W. S.), the Wellcome Trust and Biotechnology and Biological Sciences Research Council (to M. J. C. and A. R.), and the Robert A. Welch Foundation (to A. E. J.). The costs of publication of this article were defrayed in part by the payment of page charges. This article must therefore be hereby marked “advertisement” in accordance with 18 U.S.C. Section 1734 solely to indicate this fact.

§ Current address: Dept. of Zelluläre Biochemie, Max-Planck-Institut für Biochemie, D-82152 Martinsried bei München, Germany.

¶¶ To whom correspondence should be addressed: College of Medicine, Texas A&M University System Health Science Center, TAMU 1114, 116 Reynolds Medical Bldg., College Station, TX 77843-1114. Tel.: 979-862-3188; Fax: 979-862-3339; E-mail: ajohnson@medicine.tamhsc.edu.

<sup>1</sup> The abbreviations used are: TRiC, TCP-1 ring complex; eANB, N<sup>ε</sup>-(5-azido-2-nitrobenzoyl); CCT, chaperonin containing tail-less complex polypeptide 1; RNC, ribosome-nascent chain complex.

*in vivo* (12). It has been shown that multidomain proteins, such as luciferase, begin to fold cotranslationally even before the rest of the polypeptide has been synthesized and while its C terminus is still inside the ribosome (12). Furthermore, several cytosolic chaperones such as Hsp 40, Hsp 70, GIMc, and TRiC (13, 14) bind to nascent chains as they emerge from the ribosome, and it has been proposed that simultaneous protein synthesis and chaperone-mediated folding serve to maintain the nascent chains within a protected folding environment (15). This raises the possibility that chaperone interactions and nascent chain conformational states that occur during physiological folding are very different from those observed between chemically denatured, full-length proteins and purified chaperones.

To understand how TRiC functions to fold its substrates in the cell, it is important to determine how these proteins interact with the chaperonin as they emerge from the ribosome. A powerful approach to address this issue is to incorporate photoactivatable probes directly into ribosome-bound polypeptides and thereby identify by light-induced photocross-linking the proteins adjacent to the nascent chain at the time of sample illumination (photolysis). We have previously used this approach to examine the environment of nascent chains inside the ribosome (16) and during cotranslational targeting to (17), translocation across (18), and integration into (19–21) the membrane of the endoplasmic reticulum. In addition, photocross-linking experiments demonstrated that ribosome-bound actin and luciferase nascent chains interact cotranslationally with TRiC (14).

Thus, to determine whether newly synthesized chaperonin substrates interact with all or only a restricted subset of TRiC subunits, we here exploited the photocross-linking approach to identify which subunits of the hetero-oligomeric chaperonin complex are in close contact with growing polypeptide chains. Ribosome-bound actin and luciferase chains of varying lengths were cross-linked to TRiC and its subunit-specific contacts were examined after dissociating the TRiC complex and immunoprecipitating with subunit-specific antibodies under denaturing conditions. Both actin and luciferase nascent chains were found to photocross-link to at least 6 of the 8 TRiC subunits. Furthermore, actin proximity to some TRiC subunits depended upon nascent chain length, thereby suggesting that the interactions with the chaperonin changed as the chain elongates. In addition, because a single site in subdomain 2 of actin photocross-linked to multiple subunits, the actin nascent chains appear to dynamically contact and sample different TRiC subunits during the folding process. Finally, a probe photocross-links to TRiC soon after emerging from the ribosomal tunnel, so TRiC must be in extremely close proximity to the ribosomal exit site during the early stages of translation, a result that is consistent with a chaperone-dependent protected folding environment.

#### EXPERIMENTAL PROCEDURES

**Plasmids, mRNA, and tRNA**—Amber codons were introduced into plasmids coding for mouse  $\beta$ -actin and luciferase (14) using the QuikChange protocol (Stratagene), and the primary sequence of each construct was confirmed by DNA sequencing. Truncated mRNAs of defined lengths were transcribed as described elsewhere (21). Yeast  $N^{\epsilon}$ -(5-azido-2-nitrobenzoyl)-Lys-tRNA<sup>Lys</sup> ( $\epsilon$ ANB-Lys-tRNA<sup>Lys</sup>) was prepared as before (17, 21), as was the amber suppressor tRNA,  $\epsilon$ ANB-Lys-tRNA<sup>amb</sup>, which decodes an amber stop codon (21, 22).

**Radiolabeled Cell Lysate**—Human fibroblast TSA-201 cells were grown to 50% confluency, labeled overnight, and harvested as described (23) except that cells were grown in Dulbecco's modified Eagle's medium and not minimal essential media. Fractions enriched in TRiC were isolated by gel filtration on Superose 6 and then immunoprecipitated with various subunit-specific antibodies as described below.

**Translations, Photocross-linking, and Immunoprecipitations**—*In vitro* translations (26 °C, 40 min, 100  $\mu$ l) were performed in rabbit

reticulocyte lysate as before (14) in the presence of 20  $\mu$ Ci of [<sup>35</sup>S]Met and either 60 pmol of  $\epsilon$ ANB-Lys-tRNA<sup>Lys</sup> or 80 pmol of  $\epsilon$ ANB-Lys-tRNA<sup>amb</sup>. Samples were photolyzed on ice for 15 min using a 500 watt mercury arc lamp (21). After photolysis, samples were incubated (26 °C, 10 min) with 2.2  $\mu$ M RNase A, 20 mM EDTA (pH 7.4), and 14.4 mM methionine. Following clarification by sedimentation, supernatants (110  $\mu$ l) were added to 650  $\mu$ l of buffer A (20 mM HEPES (pH 7.5), 140 mM KCl, 0.1% (w/v) SDS, 1% (v/v) Nonidet P-40, 1% (w/v) sodium deoxycholate) to dissociate the TRiC complex (24). Fresh ATP was then added to a final concentration of 2 mM, and 3–14  $\mu$ l of the desired antibody were added before being rocked gently at 4 °C for 2–16 h. Affinity purified antibodies were raised against the  $\beta$ ,  $\delta$ ,  $\epsilon$ ,  $\zeta$ , and  $\theta$  TRiC subunits using a unique C-terminal peptide for each (25), whereas monoclonal antibodies against  $\alpha$  were purchased from Stressgen. After sedimentation to remove aggregates, each supernatant (750  $\mu$ l) received 20  $\mu$ l of protein A-Sepharose beads (Sigma) in buffer A containing 10% (w/v) delipidated bovine serum albumin (Sigma) before being rocked for at least 2 h at 4 °C. Beads were then pelleted, washed 3 times with 750  $\mu$ l of buffer A, and resuspended in 40  $\mu$ l of sample buffer (65 °C, 30 min). After SDS-PAGE, radioactive species were detected and quantified using a Bio-Rad FX phosphorimager.

#### RESULTS

**Experimental Approach**—McCallum and colleagues (14) previously showed that ribosome-bound actin nascent chains photocross-link to TRiC. Because the actin-TRiC photoadducts in that study were immunoprecipitated using native conditions, the TRiC subunits remained associated and it was not known which TRiC subunits were adjacent to the nascent chain.

A higher resolution view of nascent chain processing by TRiC requires both identifying any nascent chain interactions with individual TRiC subunits and also determining the nascent chain length dependence of any interactions. Translation intermediates with nascent chains of a defined length were prepared *in vitro* by translating mRNAs that were truncated in the coding region. Ribosomes halt when they reach the ends of such mRNAs, but normal termination does not occur because of the absence of a stop codon. The nascent chain therefore remains bound to the ribosome as a peptidyl-tRNA in a ribosome-nascent chain complex (RNC). Because the length of the nascent polypeptide is determined by the length of the truncated mRNA, one can examine nascent chain length dependence simply by preparing intermediates using truncated mRNAs of different lengths.

If the nascent chain binds to a particular TRiC subunit, the two polypeptides must contact and be immediately adjacent to each other. Such an interaction can then be detected using a photocross-linking approach to monitor nascent chain proximity to individual TRiC subunits at a specific time (the time of illumination). We therefore incorporated a photoactivatable probe at one or more specific sites in the nascent chain by translating the mRNA in the presence of [<sup>35</sup>S]Met and either  $\epsilon$ ANB-Lys-tRNA<sup>Lys</sup> or  $\epsilon$ ANB-Lys-tRNA<sup>amb</sup>, tRNAs that recognize either a lysine or an amber stop codon, respectively. Upon illumination, a probe in an RNC-TRiC complex will react covalently for an extremely short period of time (ns) with any protein located adjacent to the radioactive nascent chain. Whereas the formation of a particular photoadduct only proves that the nascent chain was closely juxtaposed to that TRiC subunit at the time of probe excitation, the efficiency of photocross-linking will typically be much higher between two associated proteins than between two unassociated proteins. Furthermore, by altering the position of the probe in the nascent chains, as well as the length of the nascent chains, differences in the environment of the nascent chain can be detected. This approach provides a direct means of assessing the immediate environment and interactions of the nascent chain with individual TRiC subunits at different stages during the folding process, and, in effect, provides a snapshot at a particular instant of the nas-

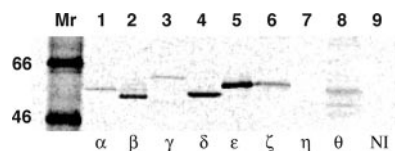


FIG. 1. **Immunoprecipitation of TRiC subunits.** Radiolabeled TRiC from human fibroblast cells were immunoprecipitated under denaturing conditions using subunit-specific antibodies as indicated. *NI*, non-immune serum.

cent chain proximity and binding to individual TRiC subunits in the RNC-TRiC complexes that comprise the sample.

**Specificity of TRiC Antibodies**—Because previous immunoprecipitations done under native conditions did not dissociate the TRiC complex into its subunits (14), the identification of subunit-specific photoadducts required immunoprecipitation conditions that dissociated the TRiC complex. Yet this approach elicited two major concerns: would the antibody-epitope association survive denaturing immunoprecipitation conditions, and would antibody specificity be compromised by cross-reactivity with other subunits under the denaturing conditions. To address these concerns, immunoprecipitation specificity and stability were assessed using radiolabeled TRiC complexes.

Human fibroblast TSA 201 cells were metabolically labeled with [<sup>35</sup>S]Met overnight and then lysed, after which the cell contents were fractionated by gel filtration chromatography. TRiC-containing fractions were identified by immunoprecipitation under native conditions with antibodies raised against the  $\beta$  subunit (data not shown). Fractions containing radiolabeled TRiC were used to identify solvent conditions that dissociated the TRiC subunits, but retained antibody binding to their epitopes. As reported previously (24), a denaturing mixed micelles buffer completely dissociated TRiC and still allowed antibodies to specifically immunoprecipitate the subunits (Fig. 1). Under these conditions (“Experimental Procedures”), 7 of the 8 antibodies raised against unique mouse C-terminal peptides (26) also recognized the corresponding human TRiC subunits (Fig. 1). However, the antibodies that recognize the mouse  $\eta$  subunit were unable to recognize the human  $\eta$  subunit (Fig. 1). Similarly, sequencing of rabbit  $\gamma$  and  $\eta$  in the region of the epitopes (GenBank<sup>TM</sup> accession numbers AAR92488 and AAR92487) revealed that there were significant differences when compared with mouse sequences. Because the mouse-specific antibodies bound weakly or not at all to the rabbit  $\gamma$  and  $\eta$  subunits,<sup>2</sup> these antibodies served as negative controls.

Because the human subunits do not contain equal numbers of methionine and cysteine residues, the observed difference in the intensities of the immunoprecipitated bands in Fig. 1 is not surprising. In addition, differences in antibody-epitope affinities probably contribute to the apparent variation in immunoprecipitation efficiencies, even though each of the polyclonal antibodies is affinity purified. But most important for this study and its goal of identifying the subunits that photocross-link to the nascent chain, six of the eight TRiC subunits were specifically immunoprecipitated under denaturing conditions that dissociated TRiC, as evidenced by the different apparent molecular masses of the subunits and the presence of only a single primary radioactive species in each lane (Fig. 1). These conditions were therefore used for all experiments reported here after titrations determined the amount of each antibody that maximized the immunoprecipitation of its cognate TRiC subunit from a defined sample size (data not shown).

**Photocross-linking of Actin Nascent Chains to Individual TRiC Subunits**—To determine which TRiC subunits are photocross-linked and hence adjacent to an actin nascent chain

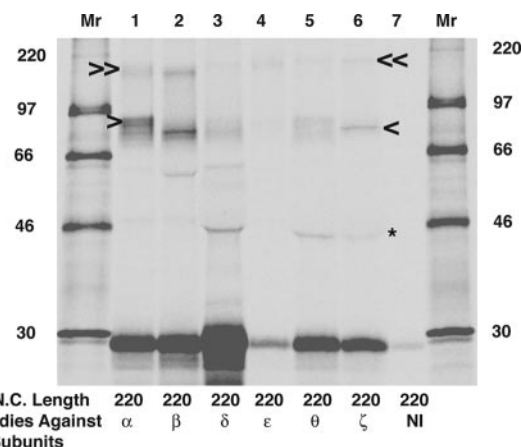


FIG. 2. **Actin nascent chain photocross-linking to TRiC subunits.** RNC-TRiC complexes containing the nascent actin 220-mer were photolyzed, and the extents of photocross-linking to different TRiC subunits were assessed by immunoprecipitation with antibodies specific for each of the subunits indicated. Photoadducts containing nascent actin and a single TRiC subunit are indicated by the *single arrowheads*, whereas photoadducts with apparent molecular masses consistent with a covalent complex between nascent actin and two TRiC subunits are indicated by the *double arrowheads*. The *asterisk* indicates radioactive material washed ahead of the IgG heavy chain. *NI*, non-immune serum.

during folding, translation intermediates (RNCs) with a 220-residue actin nascent chain (actin 220-mer) were synthesized in a rabbit reticulocyte lysate containing endogenous TRiC, [<sup>35</sup>S]Met, and  $\epsilon$ ANB-Lys-tRNA<sup>Lys</sup>. After photolysis, a sample was split into equal aliquots and immunoprecipitated under denaturing conditions before analysis by SDS-PAGE. As shown in Fig. 2, efficient photocross-linking occurred between the actin 220-mer and both the  $\alpha$  and  $\beta$  subunits of TRiC. Surprisingly, the photocross-linking of the actin 220-mer to  $\delta$  was much less efficient, even though this nascent chain contained subdomain 2 of actin. Photocross-linking of the actin 220-mer to  $\zeta$  or  $\theta$  was also weak (Fig. 2), whereas photoadduct formation between the actin 220-mer and  $\epsilon$  was visible upon longer exposure (see Fig. 6). Thus, nascent actin is in very close proximity to multiple TRiC subunits at this stage of translation and not only to  $\delta$  as concluded from the cryo-EM analysis.

We previously showed that  $\epsilon$ ANB-Lys-tRNA<sup>Lys</sup> is able to compete effectively with endogenous Lys-tRNA<sup>Lys</sup> for incorporation into protein under our *in vitro* conditions, and that an average of about one  $\epsilon$ ANB-Lys is incorporated for every four lysine codons translated (18). Because the N-terminal 220 residues of actin include 10 lysines, it is likely that each such nascent chain will contain 2 or 3 photoactivatable probes. Hence, if a single nascent chain contacts two or more TRiC subunits at the same time, then it is possible that upon photolysis a nascent chain will react covalently with more than one TRiC subunit. In fact, based on the apparent molecular masses of some immunoprecipitated photoadducts (Fig. 2, especially lane 2), the simultaneous photocross-linking of a single actin nascent chain to two TRiC subunits does occur. Thus, although the C-terminal subdomain 4 has not yet emerged from the ribosome in these RNCs, the actin nascent chain is adjacent to and probably interacts with the  $\alpha$ ,  $\beta$ ,  $\delta$ ,  $\epsilon$ ,  $\zeta$ , and  $\theta$  subunits of TRiC, and a single nascent chain is adjacent to more than one subunit at a time.

**Nascent Chain Length Dependence of Actin Photocross-linking**—Is the proximity of actin to a particular TRiC subunit dependent on the length of the nascent chain? RNCs containing nascent actin chains between 84 and 371 residues in length were photolyzed in the presence of TRiC, and the extents of nascent chain photocross-linking to 6 TRiC subunits were de-

<sup>2</sup> A. Roobol, unpublished data.



TABLE I

Actin photo-crosslinking to various TRiC subunits in the presence or absence of ATP

The symbols indicate whether a photoadduct was detected (yes, +; no, -) between a nascent actin chain of the indicated length and the indicated TRiC subunit after immunoprecipitation and analysis by SDS-PAGE. Higher resolution quantification was precluded because the large numbers of samples required many phosphorimager screens with different detection efficiencies and different exposure times because the translation efficiencies varied for different nascent chains. Each experiment was repeated a minimum of 3 times.

Nascent chain length	Photoadducts containing:					
	$\alpha$	$\beta$	$\delta$	$\epsilon$	$\zeta$	$\theta$
In the absence of apyrase						
84	-	-	-	-	-	-
133	+	+	+	+	-	-
220	+	+	+	+	+	+
303	+	+	+	+	+	+
371	+	+	+	+	+	+
In the presence of apyrase						
84	-	-	-	-	-	-
133	+	+	+	+	-	-
220	+	+	+	+	+	+
303	+	+	+	+	+	+
371	+	+	+	+	+	+

terminated by immunoprecipitation (Table I). For example, nascent actin chains of 133 residues or longer were adjacent to  $\delta$ , although the efficiency of photocross-linking varied (Fig. 3; for conciseness, only the  $\delta$  data are shown). Whereas this variation could result from a nascent chain length dependence in actin association with  $\delta$  and/or a variation in the positioning of nascent chain probes relative to the  $\delta$  subunit as the nascent chain lengthens, the important point is that the nascent chain remains in close proximity to  $\delta$  throughout the stages of folding examined.

Actin photoadducts containing two TRiC subunits were not observed until the nascent chain was 220 residues long (Fig. 3), presumably because a larger number of lysines were required in the actin nascent chain to increase the likelihood of incorporating multiple photoreactive probes into a single nascent chain. Alternatively, only the longer actin nascent chains adopt a conformation that can be simultaneously recognized by two or more subunits. These double photoadducts then continued to be formed as the nascent actin lengthened, as was true of adducts containing only the  $\delta$  subunit.

The nascent chain length dependence of actin photocross-linking to  $\alpha$ ,  $\beta$ , and  $\epsilon$  was similar to that of  $\delta$ , and the results are summarized in Table I. But photocross-linking to  $\zeta$  and  $\theta$  was detected only after the actin nascent chain reached 220 residues; no photocross-linking to  $\zeta$  and  $\theta$  was observed with RNCs containing the actin 133-mer (Table I). Thus, at an early stage of actin folding inside TRiC, the nascent chain is photocross-linked to  $\alpha$ ,  $\beta$ ,  $\delta$ , and  $\epsilon$ , but not to  $\zeta$  or  $\theta$ . Thus, it appears that nascent actin interacts differentially with the TRiC subunits at various times during the folding process.

**Nascent Chain Exposure to TRiC Subunits Is Not Dictated by ATP**—ATP is hydrolyzed as TRiC catalyzes actin folding (4). It is therefore reasonable to determine whether the presence or absence of ATP significantly alters the accessibility of the actin nascent chain to individual actin subunits, as evidenced by the presence or absence of photoadduct formation. Because ATP is required for translation, RNCs containing actin nascent chains of different lengths were first prepared using  $\epsilon$ ANB-Lys-tRNA<sup>Lys</sup>. Each sample was then split, and one-half was incubated with apyrase to hydrolyze any remaining ATP, while the other half was similarly incubated in the absence of apyrase. After photolysis, the extent of actin cross-linking to individual TRiC subunits was examined by immunoprecipitation and

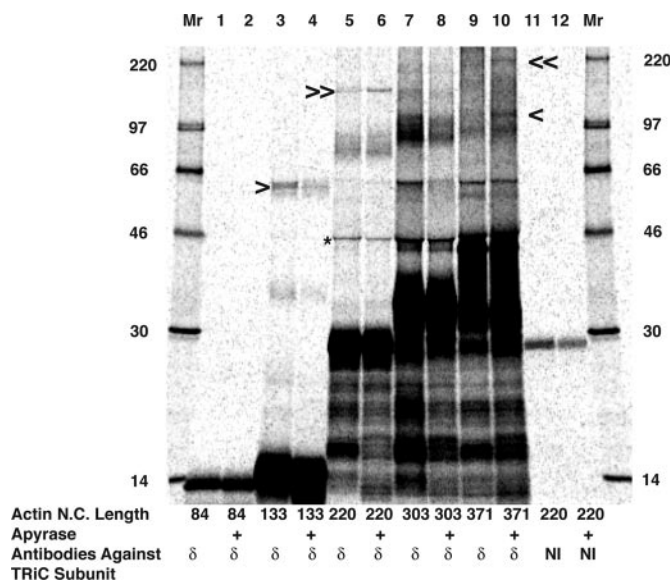


FIG. 3. Nascent chain length dependence of actin photocross-linking to  $\delta$ . RNCs containing nascent actin chains of the indicated length were photolyzed, and photoadducts between nascent actin and the  $\delta$  subunit were selected by immunoprecipitation. Samples treated with apyrase are indicated; all other samples were mock-treated. Photoadducts containing nascent actin and a single TRiC subunit are indicated by the *single arrowheads*, whereas photoadducts with apparent molecular masses consistent with a covalent complex between nascent actin and two TRiC subunits are indicated by the *double arrowheads*. The *asterisk* indicates radioactive material washed ahead of the IgG heavy chain. *NI*, non-immune serum.

SDS-PAGE. As shown in Fig. 3, the presence or absence of ATP either increased or decreased the photocross-linking yield of a particular actin nascent chain to the  $\delta$  subunit of TRiC, but did not alter the existence of nascent actin exposure to  $\delta$ . Similarly, the proximities of different nascent actin chains to  $\alpha$ ,  $\beta$ ,  $\epsilon$ ,  $\zeta$ , and  $\theta$  were not greatly influenced by the presence or absence of apyrase (Table I). Whereas nascent chain exposure to individual TRiC subunits was not sensitive to ATP under our experimental conditions, this observation may result from the continuous exposure to nucleotide during the translation incubation.

**Photocross-linking of Luciferase Nascent Chains to TRiC**—To assess the specificity of nascent chain interactions with individual TRiC subunits, photocross-linking to TRiC was examined using various lengths of nascent luciferase, another folding substrate of TRiC. Using the same experimental approach as with actin nascent chains, the  $\beta$  and  $\epsilon$  subunits of TRiC were found to photocross-link to luciferase nascent chains as short as 77 amino acids and as long as 232 amino acids either in the presence or absence of apyrase (Fig. 4). Each of these various lengths of luciferase nascent chains also photocross-linked to  $\alpha$ ,  $\delta$ ,  $\zeta$ , and  $\theta$  either in the presence or absence of apyrase (Table II).

Although each length of nascent luciferase was adjacent to each of the six TRiC subunits tested, the efficiency of nascent chain-TRiC subunit photocross-linking was not constant. This is clearly evident in Fig. 4, where the extents of photoadduct formation varied as a function of nascent chain length for both  $\beta$  (Fig. 4A) and  $\epsilon$  (Fig. 4B). Furthermore, the relative efficiency of nascent luciferase photocross-linking to  $\beta$  and  $\epsilon$  differed as the nascent chain lengthened. For example, whereas the yields of  $\beta$  and  $\epsilon$  photoadducts were similar for the luciferase 125-mer, the extents of 197-mer and 232-mer photocross-linking were much higher to  $\beta$  than to  $\epsilon$  (compare Fig. 4, A with B). These results reveal that as the nascent chain lengthens, it interacts to different extents with the individual TRiC subunits, perhaps

**FIG. 4. Photocross-linking of nascent luciferase to  $\beta$  and  $\epsilon$ .** RNCs were prepared using  $\epsilon$ ANB-Lys-tRNA<sup>L-lys</sup> and photolyzed in the presence of TRiC with or without apyrase as indicated. Photoadducts containing luciferase nascent chains of the indicated lengths and either the  $\beta$  (A) or  $\epsilon$  (B) subunits of TRiC were detected by immunoprecipitation and SDS-PAGE. Cross-linked species containing a single TRiC subunit are indicated by the *single arrowheads*, whereas species containing two TRiC subunits are indicated by *two arrowheads*. The *asterisk* indicates peptidyl-tRNA. *NI*, non-immune serum.

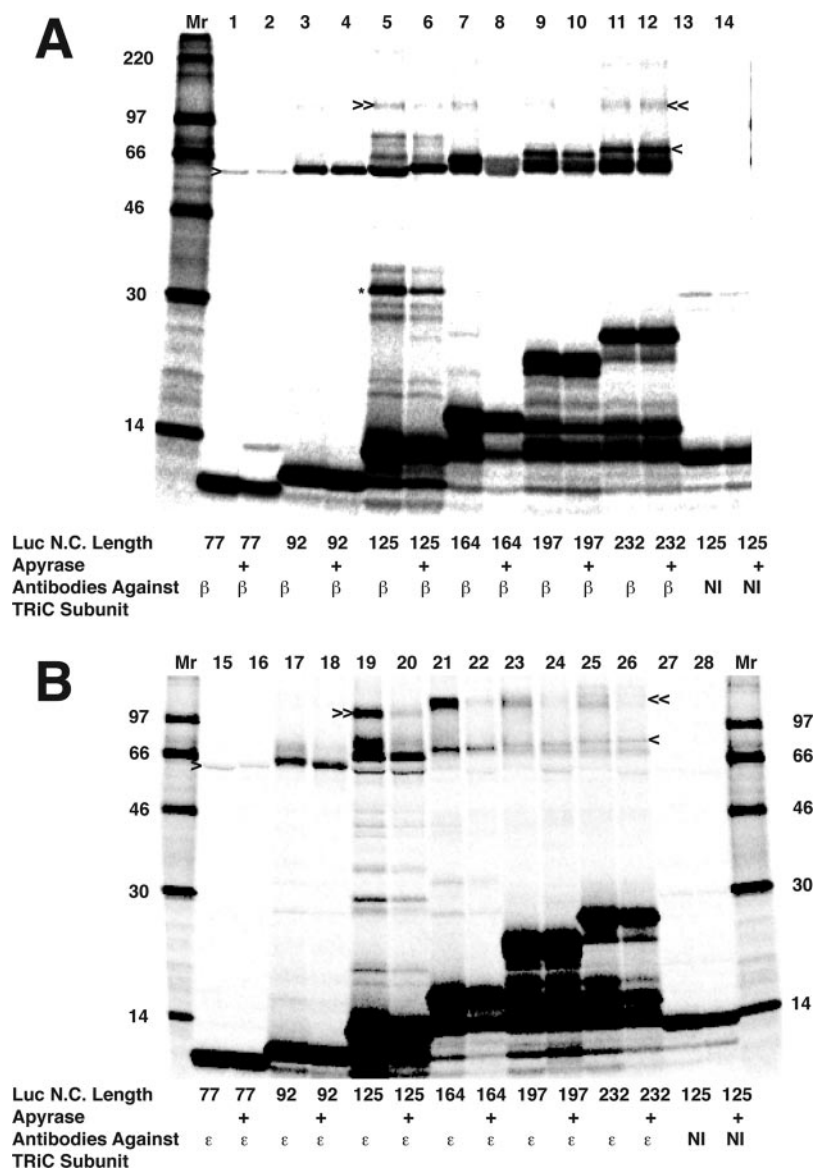


TABLE II

*Luciferase photo-crosslinking to various TRiC subunits in the presence or absence of ATP*

The symbols are defined as in the legend to Table I. Each experiment was repeated a minimum of 3 times.

Nascent chain length	Photoadducts containing:					
	$\alpha$	$\beta$	$\delta$	$\epsilon$	$\zeta$	$\theta$
In the absence of apyrase						
77	+	+	+	+	+	+
92	+	+	+	+	+	+
125	+	+	+	+	+	+
164	+	+	+	+	+	+
197	+	+	+	+	+	+
232	+	+	+	+	+	+
In the presence of apyrase						
77	+	+	+	+	+	+
92	+	+	+	+	+	+
125	+	+	+	+	+	+
164	+	+	+	+	+	+
197	+	+	+	+	+	+
232	+	+	+	+	+	+

because the subunits have differing affinities for different portions of the nascent chain. In addition, the differences noted above for  $\epsilon$  demonstrate that nascent chain exposure to and contact with individual TRiC subunits vary as the nascent

chain lengthens and folding proceeds. Because the N-terminal domain of luciferase, comprising its first 190 amino acids, folds cotranslationally, it is possible that this folding event reduces the availability of the  $\epsilon$  photocross-linking determinant in luciferase.

*A Single Probe Can Be Adjacent to More than One TRiC Subunit*—Our observation that the same actin nascent chains cross-link to multiple TRiC subunits suggests a high level of degeneracy in the specificity of the binding sites within the subunits. However, in the above experiments, a nascent chain could photocross-link to a TRiC subunit from any of several locations within the nascent chain because  $\epsilon$ ANB-Lys could be incorporated in place of any Lys in the sequence. To determine whether a single site in the actin nascent chain could interact with multiple subunits, we next introduced a photoreactive probe solely at one location in the nascent chain. To this end, a single amber stop codon was substituted into the actin coding sequence in place of the natural lysine codon at position 61, which is located within the proposed  $\delta$  binding site of subdomain 2 (9). RNCs were then synthesized *in vitro* using  $\epsilon$ ANB-Lys-tRNA<sup>amb</sup>, an amber suppressor tRNA that translates an amber stop codon and incorporates an  $\epsilon$ ANB-Lys at that location with an efficiency as high as 50% (22). Nascent chains terminated at the amber stop codon by the action of the termi-

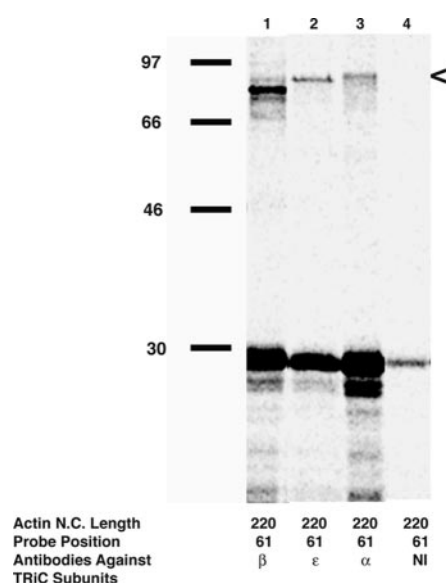


FIG. 5. Actin nascent chain photocross-linking to TRiC subunits from position 61. RNCs containing actin 220-mers with a probe at residue 61 were photolyzed in the presence of TRiC and immunoprecipitated as indicated. Photoadducts are identified by the arrowheads. NI, non-immune serum.

nation factor do not contain a probe and hence do not influence photocross-linking results; only intermediates that incorporate the modified lysine would continue translation to the end of the truncated mRNA to yield a radioactive nascent chain of the desired length.

To determine whether the probe at this single location photocross-links to several TRiC subunits, a sample of actin 220-mer RNCs with the probes at position 61 was therefore photolyzed, and equal aliquots of the sample were immunoprecipitated with anti-subunit antibodies. These actin nascent chains photocross-linked to  $\beta$ ,  $\epsilon$ , and  $\alpha$  (Fig. 5), with the cross-links being most intense with the  $\beta$  subunit (Fig. 5). Thus, at this stage of protein folding inside TRiC, this particular segment in the actin nascent chains is in contact with at least three different TRiC subunits.

To assess whether this apparent promiscuity in subunit binding reflects the specificity of nascent chain-TRiC interactions during the course of actin folding, the dependence of photocross-linking on both nascent chain length and probe location were examined. The data summarized in Table III demonstrate that in a sample of RNC-TRiC complexes, three different TRiC subunits ( $\alpha$ ,  $\beta$  and  $\epsilon$ ) were each exposed (photocross-linked) to each of five different sites along the nascent actin chain when it was 133 residues or longer. Thus, once the nascent chain probes have emerged from the ribosome, five different actin sequences are simultaneously adjacent to three different TRiC subunits in a population of RNC-TRiC complexes as the nascent chain is lengthened from 133 to 371 residues.

*Site-specific Photocross-linking of Nascent Actin to  $\beta$* —To characterize further the exposure of specific sites in the nascent chain to a given subunit, we next substituted a single amber stop codon into the actin coding sequence in place of one of the natural lysine codons at positions 18, 50, 61, 68, or 84. Because actin containing a single probe at position 61 photocross-linked most strongly to subunit  $\beta$  (Fig. 5), we examined the effect of positioning the probe at these positions on the photoadduct yield with this subunit.

Five samples of actin 220-mer RNCs were prepared that differed only in the location of the photoactivatable probe in the nascent chain: at positions 18, 50, 61, 68, or 84. Upon photolysis

TABLE III

Exposure of specific residues in nascent actin chains of different lengths to TRiC subunits

The symbols are defined as in the legend to Table I. Most experiments were repeated 3 times; some with lengths between 177 and 337 were done only once if photoadduct formation was detected.

Nascent chain length	Probe located at residue:				
	18	50	61	68	84
Photoadducts to the TRiC $\beta$ subunit					
60	–	ND <sup>a</sup>			
84	+	+	+	ND	
133	+	+	+	+	+
177	+	+	+	+	+
220	+	+	+	+	+
260	+	+	+	+	+
303	+	+	+	+	+
337	+	+	+	+	+
371	+	+	+	+	+
Photoadducts to the TRiC $\alpha$ subunit					
60	–	–			
84	–	–	–	–	
133	+	+	+	+	+
177	+	+	+	+	+
220	+	+	+	+	+
260	+	+	+	+	+
303	+	+	+	+	+
337	+	+	+	+	+
371	+	+	+	+	+
Photoadducts to the TRiC $\epsilon$ subunit					
60	–	–			
84	–	–	–	–	
133	+	+	+	+	+
177	+	+	+	+	+
220	+	+	+	+	+
260	+	+	+	+	+
303	ND	+	+	+	+
337	ND	+	+	+	+
371	+	+	+	+	+

<sup>a</sup> ND, not done.

in the presence of TRiC, each actin 220-mer derivative was found to photocross-link to the  $\beta$  subunit of TRiC, although with different efficiencies (Fig. 6A). It therefore appears that at this stage of actin folding, residues 50, 61, and 68 are exposed equally to  $\beta$ , whereas residues 18 and 84 are adjacent to  $\beta$  much less frequently than are the other actin sites.

The nascent chain length dependence of photocross-linking  $\beta$  from each of these actin positions was then examined. Whereas 84-residue nascent chains photocross-linked only weakly to  $\beta$ , each probe location in actin nascent chains between 133 and 337 residues in length was adjacent to  $\beta$  (Fig. 6, B–F). Because each of the five actin residues was able to contact  $\beta$  in the TRiC complex as the nascent chain increased in length by a minimum of 204 residues, the nascent chain does not appear to localize at a stable site(s) within the TRiC cavity during the folding process. The dramatic decrease in the photocross-linking to  $\beta$  of all probe locations in the 371-mer (when nascent actin is almost full-length) except 18 may be because of the cotranslational formation of folded structures in the N-terminal portion of actin that contains the probe sites.

*TRiC Is in Close Proximity to the Ribosomal Exit Site When Bound to the Nascent Chain*—TRiC associates with nascent chains as they emerge from the ribosomal nascent chain tunnel, and the data in Fig. 6F (lane 39) show that a probe at position 84 in a 133-residue nascent chain photocross-links to the  $\beta$  subunit of TRiC. Thus, an amino acid in the nascent chain located only 49 residues from the ribosomal P site is adjacent to TRiC. How close can TRiC get to the ribosome as it binds and sequesters the nascent chain? RNCs containing a 125-residue actin nascent chain with a probe at position 84 were prepared, photolyzed, and found by immunoprecipitation to react covalently with TRiC  $\beta$  (Fig. 7). A probe in the nascent chain only



**FIG. 6. Photocross-linking of TRiC  $\beta$  from different actin sites.** A, RNCs containing actin 220-mers with a single  $\epsilon$ ANB-Lys at positions 18, 50, 61, 68, or 84 were photolyzed, and photoadducts containing the  $\beta$  subunit were detected by immunoprecipitation and are indicated by the *arrowheads*. Photocross-linking to  $\beta$  of actin nascent chains of the indicated lengths with probes located only at residues 18 (B), 50 (C), 61 (D), 68 (E), or 84 (F). Immunoprecipitated photoadducts are indicated by *arrowheads*. Samples in lanes 6, 15, 23, 31, 38, and 45 were immunoprecipitated with non-immune serum (NI).

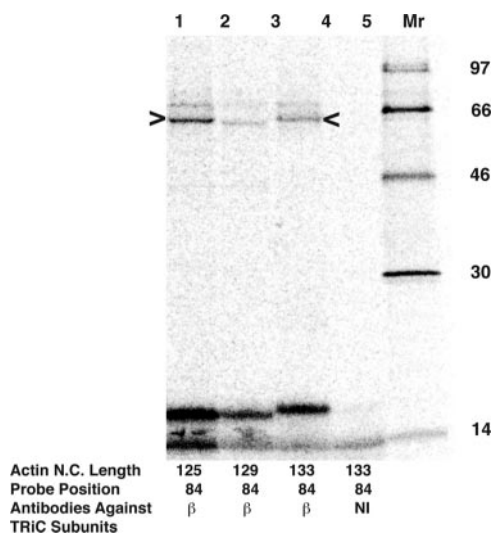
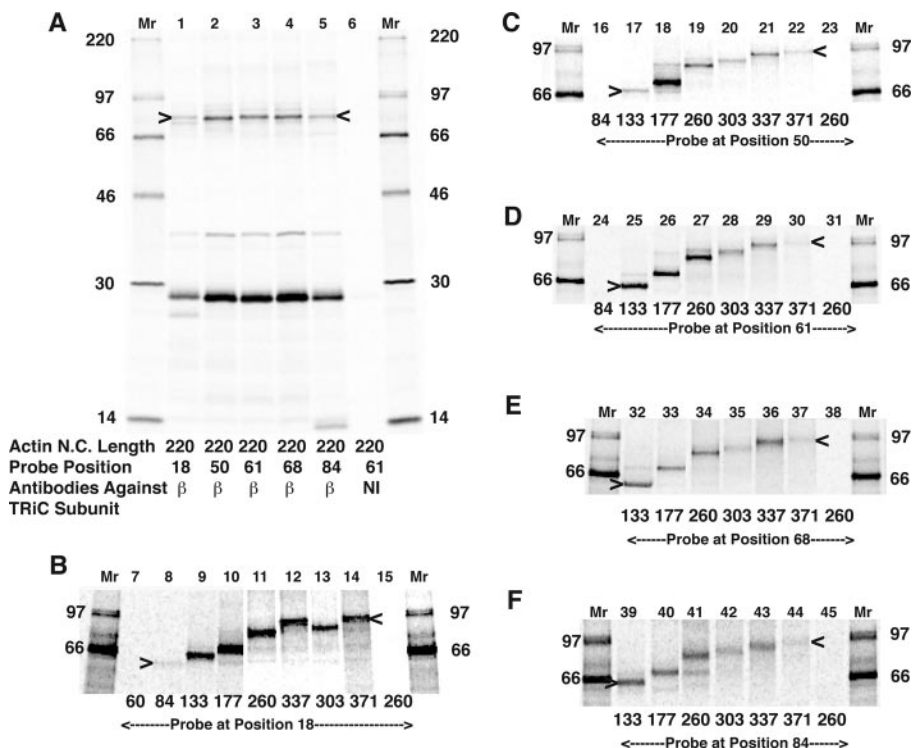


**FIG. 7. Proximity of TRiC to the ribosomal tunnel exit site.** RNCs containing actin nascent chains of 125, 129, or 133 residues with a probe at position 84 were photocross-linked to TRiC, and photoadducts to  $\beta$  detected by immunoprecipitation are shown (*arrowheads*). NI, non-immune serum.

41 residues from the ribosomal P-site can therefore react covalently with TRiC.

#### DISCUSSION

Although the mechanism by which a chaperonin catalyzes the folding of a nascent chain as it is being synthesized by the ribosome has not yet been elucidated, it is presumed to involve the entry of the nascent chain into the chaperonin cavity and then a series of interactions with some or all of the chaperonin subunits to yield a folded protein or protein domain. But in actual fact, few experimental data bear directly on the nature and specificity of physiological (ribosome-bound) nascent chains with chaperonin subunits, other than that those interactions are somehow facilitated by ATP hydrolysis. We therefore decided to determine the answers to five critical questions that would iden-

tify important and fundamental properties of co-translational processing of the nascent chain by a chaperonin. Is a nascent chain sequence exposed to all chaperonin subunits, or does it contact only a select few? Does nascent chain exposure to a chaperonin subunit change as translation and folding proceed? Can a nascent chain interact with two chaperonin subunits simultaneously? Do different nascent chains interact similarly with the chaperonin? How soon does the nascent chain interact with individual chaperonin subunits?

These questions were addressed experimentally by incorporating one or more photoactivatable probes into nascent chains of actin and firefly luciferase as they were being synthesized by a ribosome. Each sample contained a population of RNC complexes in which each nascent chain had the same defined length and a probe(s) located at the same defined location(s). Because TRiC associates with these nascent chains during their translation (14), we then illuminated each RNC-TRiC sample to initiate the photocross-linking of the nascent chain to any nearby chaperonin subunit and thereby provide a nearly instantaneous snapshot of nascent chain proximity to individual subunits at the chosen stage of folding. Were the nascent chain bound tightly to only one or a few subunits, then we would expect to obtain only a limited number of nascent chain-TRiC subunit photoadducts. Yet we observed something very different.

The comprehensive investigation carried out in this study and summarized in Tables I–III reveals that actin nascent chains of 220 residues or longer are adjacent to at least 6 of the 8 TRiC subunits at the time of photolysis (Figs. 2 and 5, Tables I and III). More precisely, whereas a single nascent chain may be simultaneously adjacent to 6 subunits, at least a fraction of the nascent chain population in the sample is adjacent to each of the 6 subunits at any given time. Similarly, nascent luciferase chains of 77 residues or longer are adjacent to 6 of the 8 TRiC subunits at the time of photolysis (Fig. 4; Table II). Furthermore, this apparent non-selectivity in the distribution of nascent chains between TRiC subunits was maintained as the actin and luciferase nascent chains lengthened to 371 and 232 residues, respectively (Tables I–III, Figs. 3, 4, and 6).

Because the photocross-linking approach did not identify a low number of discrete, stable, and reproducible nascent chain photoadducts with specific TRiC subunits, it is clear that the nascent chain does not occupy a fixed location within the cavity where it is bound to only a select few of the subunits. In fact, even when an actin nascent chain contained only a single probe (at each of five different sites) and its flanking sequence might be expected to direct that portion (sequence) of the nascent chain to bind and photocross-link to only one or two subunits, the singly labeled nascent chains photocross-linked to several TRiC subunits (Table III, Fig. 5). Hence, there is significant overlap in the nascent chain binding specificities of the individual subunits. These data therefore lead overwhelmingly to the conclusion that any nascent chain within the chaperonin cavity is in a dynamic state, is exposed transiently to each of the TRiC subunits, and moves from one subunit to another within the cavity, irrespective of the length (folding state) of the nascent chain.

Having said that, it is also clear from our data that nascent chain-TRiC subunit interactions are not completely non-selective and promiscuous. This is evident from variations in the efficiency of nascent chain- $\beta$  photocross-linking as the length of the nascent chain increases and as the position of the probe varies (Fig. 6), as well as from the different efficiencies of actin 220-mer photocross-linking to various TRiC subunits (Fig. 2). Thus, it seems likely that there are different affinities of individual TRiC subunits for specific nascent chain sequences, and that the higher affinity interactions will necessarily lead to higher photocross-linking efficiencies and greater photoadduct formation. Yet the broad distribution of photoadduct identities suggests that such affinity differences are relatively small and only modulate to a limited extent the duration of subunit-substrate interactions.

This view of nascent chain-TRiC interactions is at odds with the currently proposed model for substrate-TRiC interactions, which holds that a particular substrate polypeptide interacts with specific subunits within the cavity. The latter opinion originated largely from cryo-EM data that appeared to show that chemically unfolded actin polypeptides (containing essentially the same residues examined in this study) assumed a stably folded and highly structured conformation within the cavity, and was in close proximity to only two TRiC subunits,  $\alpha$  and either  $\beta$  or  $\epsilon$  (9). In contrast, our results suggest that newly made actin polypeptides contact multiple subunits in the TRiC complex. So why do the photocross-linking and cryo-EM analyses yield different conclusions? We believe that the discrepancy originates both from the different techniques employed and from the nature of the samples analyzed.

Whereas each photocross-linking experiment reported here in the figures and Tables detects and analyzes more than  $10^{11}$  probe-containing nascent chains per sample, Llorca *et al.* (9) included less than 2500 total particles in their image reconstruction analyses (9). To obtain high-resolution images, cryo-EM particle reconstructions must reduce the number of structurally diffuse and ill-defined particles included in their analyses. Because unfolded actin polypeptides inside TRiC particles are not well defined and would decrease resolution, such images are not included in the analysis, thereby biasing the final result by this pre-selection of data. Thus, in addition to the obvious differences in the nature of the data collected in cryo-EM and photocross-linking experiments, the two studies differ greatly in the total number of substrate-TRiC complexes examined and in the stringency of inclusion of all substrate-TRiC complexes in the analysis. It should also be noted that whereas cryo-EM reconstructions indicate that TRiC-bound actin is in a highly compacted conformation, biochemical analysis of TRiC-

actin complexes indicate that most actin chains are in a protease-sensitive, relatively unstructured conformation (11).

Another major difference between the two studies involves the substrate. The C terminus of each nascent chain in the photocross-linking studies is covalently bound to a peptidyl-tRNA in the ribosomal P site, and hence each nascent chain is tethered to the peptidyltransferase center far inside the ribosome. Thus, in the photocross-linking studies, every nascent chain substrate must have its C-terminal end extending out of the entrance to the TRiC cavity and into the ribosome, whereas the N-terminal end of the nascent chain is free to sample different conformations and folding intermediates. In contrast, the substrates examined in the cryo-EM study are able to insert fully into the chaperonin cavity, and their freedom to sample different conformations and fold is not restricted by having one end extending through the cavity entrance and fixed in location somewhere outside the chaperonin. Given the non-physiological nature of the latter samples, it is not clear to what extent they mirror the conformational states and opportunities that occur and exist *in vivo*. Importantly, whereas only a subfraction of the chemically denatured actin is correctly folded by TRiC, suggesting that many of the actin chains interact in a non-productive conformation (*e.g.* Refs. 11 and 27), most of the newly translated actin is efficiently and rapidly folded by TRiC (*e.g.* Refs. 15 and 28). Thus the folding efficiencies and folding intermediates of the *de novo* folding process probably differ significantly from those observed using purified components.

Whereas the photocross-linking data indicate that at any given time there are a plethora of different nascent chain-subunit interactions and structures present in a population of RNC-TRiC complexes, it is also important to note that the photocross-linking experiments reveal some structural constraints. For example, whereas an 84-residue actin does not react covalently with any TRiC subunit and a 220-residue actin reacts covalently with all six of the TRiC subunits examined, a 133-residue actin reacts covalently with only the  $\alpha$ ,  $\beta$ ,  $\delta$ , and  $\epsilon$  subunits (Table I). Thus, it appears that when nascent actin first enters the TRiC cavity, the short nascent chain is not detectably exposed to the  $\theta$  and  $\zeta$  subunits. Similarly, when a photoreactive probe is positioned at residue 18 in an 84-residue long nascent actin, this probe is able to react covalently with the  $\beta$  subunit, but not with the  $\alpha$  and  $\epsilon$  subunits (Table III). Based on these differential effects that depend on nascent chain length, it would appear that there is a preferred interaction pathway for the nascent chain as it enters the chaperonin, although more data are necessary to clarify the nature of this putative pathway. Because the interactions with individual TRiC subunits differed for actin and luciferase nascent chains, such a pathway may vary depending upon the substrate as each nascent chain proceeds sequentially through a series of folding states and intermediates within the cavity that may alter probe exposure to a particular subunit.

Three other points should be noted. First, the detection of photoadducts containing two TRiC subunits (Figs. 2 and 3) indicates that a single nascent chain can contact two different subunits at the same time. It seems likely that the longer nascent chains could simultaneously contact even more subunits, but this has yet to be demonstrated experimentally. Second, we observed ATP-dependent differences in the photocross-linking efficiencies of various nascent chains to different subunits, but no clear and consistent pattern emerged (*e.g.* not all efficiencies increased in the presence of ATP). Hence, we cannot as yet ascertain the basis of the observed ATP dependence of nascent chain exposure to the different TRiC subunits. Third, as we have noted previously (14), TRiC is able to associate with the nascent chain soon after it emerges from its



ribosomal exit site. Here we have found that a 133-residue actin with a probe at position 84 is able to photocross-link to the TRiC  $\alpha$ ,  $\beta$ , and  $\epsilon$  subunits (Table III), whereas a 125-residue actin with a probe at 84 can photocross-link the  $\beta$  subunit (Fig. 7). Thus, a probe located only 41 nascent chain residues from the ribosomal P site is able to photocross-link to TRiC. We have shown recently using fluorescence resonance energy transfer between two different fluorophores incorporated into the same nascent chain that soluble proteins are approximately fully extended within the nascent chain tunnel (16). This result would indicate that the probe is located about 143 Å ( $41 \times 3.5$  Å/fully extended residue) from the P site when cross-linking occurs, and because the length of the nascent chain tunnel is on the order of 100 Å, it would appear that the TRiC  $\beta$  subunit is located within  $\sim 40$  Å of the ribosomal exit site in the co-translational RNC-TRiC complex.

In summary, the extensive analysis of nascent chain proximity to individual TRiC subunits performed here suggests that nascent polypeptides contact multiple chaperonin subunits upon emerging from the ribosome. Multiple TRiC subunits appear to engage the same portion of the polypeptide, albeit with different affinities. Thus, in contrast to the static view of highly specific substrate-chaperonin interactions that currently prevails, our experiments provide experimental support for dynamic interactions between the polypeptide substrate and the chaperonin. Whereas different subunits exhibit some specificity in substrate binding, the full range of nascent chain-TRiC interactions at each stage of folding under physiological conditions exhibits remarkable plasticity.

*Acknowledgments*—We are grateful to Drs. Christine McCallum and Jason Young, as well as current and former members of the Johnson lab, for helpful discussions.

## REFERENCES

1. Bukau, B., and Horwich, A. L. (1998) *Cell* **92**, 351–366
2. Frydman, J. (2001) *Annu. Rev. Biochem.* **70**, 603–647
3. Hartl, F. U., and Hayer-Hartl, M. (2002) *Science* **295**, 1852–1858
4. Spiess, M., Meyer, A. S., Reissmann, S., and Frydman, J. (2004) *Trends Cell Biol.* **14**, 598–604
5. Hartl, F. U. (1996) *Nature* **381**, 571–580
6. Ying, B.-W., Taguchi, H., Kondo, M., and Ueda, T. (2005) *J. Biol. Chem.* **280**, 12035–12040
7. Gutsche, I., Essen, L. O., and Baumeister, W. (1999) *J. Mol. Biol.* **293**, 295–312
8. Liou, A. K., and Willison, K. R. (1997) *EMBO J.* **16**, 4311–4316
9. Llorca, O., McCormack, E. A., Hynes, G., Grantham, J., Cordell, J., Carrascosa, J. L., Willison, K. R., Fernandez, J. J., and Valpuesta, J. M. (1999) *Nature* **402**, 693–696
10. Llorca, O., Martin-Benito, J., Grantham, J., Ritco-Vonsovici, M., Willison, K. R., Carrascosa, J. L., and Valpuesta, J. M. (2001) *EMBO J.* **20**, 4065–4075
11. Meyer, A. S., Gillespie, J. R., Walther, D., Millet, I. S., Doniach, S., and Frydman, J. (2003) *Cell* **113**, 369–381
12. Frydman, J., Erdjument-Bromage, H., Tempst, P., and Hartl, F. U. (1999) *Nat. Struct. Biol.* **6**, 697–705
13. Frydman, J., Nimmegern, E., Ohtsuka, K., and Hartl, F. U. (1994) *Nature* **370**, 111–117
14. McCallum, C. D., Do, H., Johnson, A. E., and Frydman, J. (2000) *J. Cell Biol.* **149**, 591–601
15. Thulasiraman, V., Yang, C.-F., and Frydman, J. F. (1999) *EMBO J.* **18**, 85–95
16. Woolhead, C., McCormick, P. J., and Johnson, A. E. (2004) *Cell* **116**, 725–736
17. Krieg, U. C., Walter, P., and Johnson, A. E. (1986) *Proc. Natl. Acad. Sci. U. S. A.* **83**, 8604–8608
18. Krieg, U. C., Johnson, A. E., and Walter, P. (1989) *J. Cell Biol.* **109**, 2033–2043
19. Thrift, R. N., Andrews, D. W., Walter, P., and Johnson, A. E. (1991) *J. Cell Biol.* **112**, 809–821
20. Do, H., Falcone, D., Lin, J., Andrews, D. W., and Johnson, A. E. (1996) *Cell* **85**, 369–378
21. McCormick, P. J., Miao, Y., Shao, Y., Lin, J., and Johnson, A. E. (2003) *Mol. Cell* **12**, 329–341
22. Flanagan, J. J., Chen, J.-C., Miao, Y., Shao, Y., Lin, J., Bock, P. E., and Johnson, A. E. (2003) *J. Biol. Chem.* **278**, 18628–18637
23. Feldman, D. E., Thulasiraman, V., Ferreyra, R. G., and Frydman, J. (1999) *Mol. Cell* **4**, 1051–1061
24. Hynes, G. M., and Willison, K. R. (2000) *J. Biol. Chem.* **275**, 18985–18994
25. Roobol, A., Grantham, J., Whitaker, H. C., and Carden, M. J. (1999) *J. Biol. Chem.* **274**, 19220–19227
26. Hynes, G., Kubota, H., and Willison, K. R. (1995) *FEBS Lett.* **358**, 129–132
27. Tian, G., Vainberg, I. E., Tap, W. D., Lewis, S. A., and Cowan, N. J. (1995) *Nature* **375**, 250–253
28. Frydman, J., and Hart, F. U. (1996) *Science* **272**, 1497–1502